Initial formation of zebrafish brain ventricles occurs independently of circulation and requires the *nagie oko* and *snakehead/atp1a1a.1* gene products

Laura Anne Lowery[1,2] and Hazel Sive[1,2,*]

[1]Whitehead Institute for Biomedical Research, Nine Cambridge Center, Cambridge, MA 02142, USA
[2]Massachusetts Institute of Technology, 77 Massachusetts Avenue, Cambridge, MA 02139-4307 USA
*Author for correspondence (e-mail: sive@wi.mit.edu)

Accepted 15 February 2005

Development 132, 2057-2067
Published by The Company of Biologists 2005
doi:10.1242/dev.01791

Summary

The mechanisms by which the vertebrate brain develops its characteristic three-dimensional structure are poorly understood. The brain ventricles are a highly conserved system of cavities that form very early during brain morphogenesis and that are required for normal brain function. We have initiated a study of zebrafish brain ventricle development and show here that the neural tube expands into primary forebrain, midbrain and hindbrain ventricles rapidly, over a 4-hour window during mid-somitogenesis. Circulation is not required for initial ventricle formation, only for later expansion. Cell division rates in the neural tube surrounding the ventricles are higher than between ventricles and, consistently, cell division is required for normal ventricle development. Two zebrafish mutants that do not develop brain ventricles are *snakehead* and *nagie oko*. We show that *snakehead* is allelic to *small heart*, which has a mutation in the Na^+K^+ ATPase gene *atp1a1a.1*. The *snakehead* neural tube undergoes normal ventricle morphogenesis; however, the ventricles do not inflate, probably owing to impaired ion transport. By contrast, mutants in *nagie oko*, which was previously shown to encode a MAGUK family protein, fail to undergo ventricle morphogenesis. This correlates with an abnormal brain neuroepithelium, with no clear midline and disrupted junctional protein expression. This study defines three steps that are required for brain ventricle development and that occur independently of circulation: (1) morphogenesis of the neural tube, requiring *nok* function; (2) lumen inflation requiring *atp1a1a.1* function; and (3) localized cell proliferation. We suggest that mechanisms of brain ventricle development are conserved throughout the vertebrates.

Key words: Brain ventricle formation, Brain structure, Circulation, Morphogenesis, Zebrafish, Lumen inflation, *snakehead* (*snk*), *nagie oko* (*nok*), Neural tube, Epithelial polarity, MAGUK family, Na^+K^+ ATPase, *atp1a1a.1*

Introduction

The vertebrate brain has a characteristic and complex three-dimensional structure, the development of which is not well understood. Brain morphogenesis begins during, and continues subsequent to, neural tube closure. One aspect of brain structure that is highly conserved throughout the vertebrates is the brain ventricular system.

The brain ventricles are cavities lying deep within the brain, which contain cerebrospinal fluid (CSF) and form a circulatory system in the brain (Cushing, 1914; Milhorat et al., 1971; Pollay and Curl, 1967). This system is believed to have essential roles in brain function, including waste removal, nutrition, protection and pressure equilibration (Novak et al., 2000). Recent evidence suggests that CSF directly regulates neuronal proliferation in the embryonic brain and is part of a non-synaptic communication system in the adult (Miyan et al., 2003; Owen-Lynch et al., 2003; Skinner and Caraty, 2002). In addition, certain neurons send processes into the ventricular space, suggesting that their activity may be connected with regulating CSF homeostasis (Vigh and Vigh-Teichmann, 1998). CSF contains hormones, proteoglycans and ions, and its composition varies between ventricles and over time, suggesting a changing function for the ventricles during development (Alonso et al., 1998; Skinner and Caraty, 2002). Abnormalities in brain ventricle structure can lead to hydrocephaly, one of the most common birth defects (McAllister and Chovan, 1998; Rekate, 1997), and abnormal brain ventricle size and development have been correlated with mental health disorders such as autism and schizophrenia (Hardan et al., 2001; Kurokawa et al., 2000).

While the adult brain ventricles have a complex shape, the embryonic brain begins as a simple tube, the lumen of which forms the brain ventricles. During and after neurulation, the anterior neural tube dilates in three specific locations to form the future forebrain, midbrain and hindbrain ventricles (also called brain vesicles). This dilation pattern is highly conserved in all vertebrates. Elegant studies in chick embryos have shown that intraluminal pressure resulting from the accumulation of CSF inside the brain ventricles is necessary for normal brain ventricle expansion and cell proliferation (Desmond, 1985; Desmond and Levitan, 2002), and levels of proteoglycans such as chondroitin sulfate affect this process (Alonso et al., 1998;

Development

Development

Alonso et al., 1999). However, the molecular mechanisms underlying brain ventricle formation are almost completely unknown. This has been due, in part, to lack of a genetic model in which early brain ventricle development could be observed.

We have considered whether the zebrafish is a good model for analyzing brain morphogenesis. One issue is whether the zebrafish neural tube forms by a similar mechanism to the amniote neural tube, as teleost neurulation involves formation of a solid neural keel, whereas amniote and amphibian neurulation involves rolling of the neuroepithelium into a tube. Our evaluation of the primary literature clearly indicates that teleost, amniote and amphibian neurulation occur via fundamentally similar topological mechanisms, supporting the use of zebrafish as a model for brain morphogenesis (Lowery and Sive, 2004). We therefore initiated a project to analyze brain ventricle formation using the zebrafish as a model. Brain ventricle mutants have been identified in several mutagenesis screens (Guo et al., 1999; Jiang et al., 1996; Schier et al., 1996); however, most have not been studied further.

In this study, we characterize normal brain ventricle formation in the zebrafish, and examine in detail the phenotypes of two severe brain ventricle mutants, *nagie oko* and *snakehead*. Our data define a series of steps necessary for brain ventricle development and demonstrate the utility of the zebrafish as a system for in-depth analysis of this process.

Materials and methods

Fish lines and maintenance

Danio rerio fish were raised and bred according to standard methods (Westerfield, 1995). Embryos were kept at 28.5°C and staged according to Kimmel et al. (Kimmel et al., 1995). Times of development are expressed as hours post-fertilization (hpf).

Lines used were: Tübingen Long Fin, sih^{tc300B} (Sehnert et al., 2002), snk^{to273a} (Jiang et al., 1996), nok^{wi83} (Wiellette et al., 2004), snk^{to273a}; nok^{wi83}, slh^{m291} (Yuan and Joseph, 2004). Double mutant snk^{to273a}; nok^{wi83} were constructed using standard genetic techniques. To genotype double mutant embryos, PCR analysis of *nok* and morphology analysis for *snk* was used. After sorting *snk* mutant embryos phenotypically, the heads from each individual were removed, fixed in 2% paraformaldehyde, 1% glutaraldehyde, and processed for sectioning as described below. The remaining body was digested with proteinase K (1 mg/ml) in lysis buffer (10 mmol/l Tris pH 8, 1 mmol/l EDTA, 0.3% Tween-20, 0.3% NP40) and used for PCR genotyping for the *nok* locus. Because nok^{wi83} has a retroviral insertion in the *nok* gene, mutant individuals could be identified by PCR. Primers used: nokf 5′-GGTGAGCTGCCACTTTTCGGACA-3′, nokr 5′-TAGCGACCCGTCACATAACA-3′, retroviral-specific primer 5′-CCATGCCTTGCAAAATGGCGTTACTTAAGC-3′ (MWG Biotech). To identify the wild-type allele, nokf and nokr primers were used. To identify the nok^{wi83} allele, nokf and insertion primers were used.

Brain ventricle imaging

Embryos were anesthetized in 0.1 mg/ml Tricaine (Sigma) dissolved in embryo medium (Westerfield, 1995) prior to injection and imaging. The hindbrain ventricle was micro-injected with 2-10 nl dextran conjugated to Rhodamine or Texas Red (5% in 0.2 mol/l KCl, Sigma), the fluorescent molecule then diffused through the brain cavities, and micrographs were taken with light and fluorescent illumination within 10 minutes of injection. These two images were superimposed in Photoshop 6 (Adobe). Injected embryos survive and develop normally. Comparisons of injected and non-injected brains show ventricle size is not perturbed by injection.

Live confocal imaging

Bodipy ceramide (Fl C5, Molecular Probes) was dissolved in DMSO to a stock concentration of 5 mmol/l. Embryos were soaked in 50 nmol/l bodipy ceramide solution overnight in the dark. The embryos were then washed, dechorionated and placed in wells in 1% agarose for confocal microscopy. Confocal imaging was performed using a Zeiss LSM510 laser-scanning microscope, using standard confocal imaging techniques (Cooper et al., 1999). Confocal images were analyzed using LSM software (Zeiss) and Photoshop 6.0 (Adobe).

Histology

Embryos were fixed in 2% paraformaldehyde, 1% glutaraldehyde in PBS overnight at 4°C, then washed in PBS, dechorionated, dehydrated and embedded in plastic according to the manufacturer's instructions (JB-4 Plus Embedding Kit, Polysciences). Sections 5-8 μm were cut on Leica RM2065 microtome and stained with hematoxylin and eosin using standard staining methods (Polysciences).

Immunohistochemistry

For labeling with anti-phosphohistone H3 antibody, anti-Nagie oko antibody and phalloidin-Texas Red, embryos were fixed in 4% paraformaldehyde for 2 hours at room temperature, then rinsed in PBS and dechorionated. For labeling with anti-β-catenin polyclonal antibody, anti-occludin polyclonal antibody and anti-alpha Na^+K^+ ATPase a6F antibody, dechorionated embryos were fixed in Dent's fixative (80% methanol, 20% DMSO) for 2 hours at room temperature, then rinsed in PBS (Dent et al., 1989). Blocking was done for 4 hours at room temperature in 0.5% Triton X, 4% normal goat serum, in phosphate buffer. Whole-mount immunostaining was carried out using anti-phosphohistone H3 rabbit polyclonal antibody (Upstate Biotechnology, 1:800), anti-β-catenin rabbit polyclonal antibody (Zymed Laboratories, 1:50), anti-occludin rabbit polyclonal antibody (Zymed Laboratories, 1:50), anti-Nagie oko rabbit polyclonal antibody (Wei and Malicki, 2002) (1:500), and mouse monoclonal antibody alpha6F, raised against chicken alpha1 subunit of Na^+K^+ ATPase (Takeyasu et al., 1988) (1:100), which was obtained from the Developmental Studies Hybridoma Bank. Goat anti-rabbit IgG Alexa Fluor 488 (Molecular Probes, 1:500) and goat anti-mouse Alexa Fluor 488 (Molecular Probes, 1:500) were used as secondary antibodies. Phalloidin conjugated to Texas Red (Sigma, 1:1000) was used to label actin filaments. Brains were flat-mounted in glycerol and imaged with a confocal microscope. For transverse sections, brains were embedded in 4% low melting agarose and sectioned with a vibratome (200 μm sections) before confocal imaging.

For cell proliferation quantification, phosphohistone H3-labeled cells in each z-series of the midbrain-hindbrain boundary and hindbrain regions were counted and averaged. Average z-series areas of the regions were measured using Scion Image software (Scion Corporation), and by determining the approximate area occupied by each cell, total cell number and the percentage of labeled cells in each region were calculated. To determine the statistical difference among different regions at the same time point, statistical analyses were performed using a paired sample *t*-test with SPSS 13.0 for Windows (SPSS). Cell death quantification was performed similarly, using an ANOVA test for comparison of multiple groups. $P<0.05$ was considered significant.

Cell death labeling

DNA fragmentation during apoptosis was detected by the TUNEL method, using 'ApopTag' kit (Chemicon). Embryos were fixed in 4% paraformaldehyde in PBS for 2 hours, then rinsed in PBS and dechorionated. Embryos were dehydrated to 100% ethanol, stored at –20°C overnight, then rehydrated in PBS. Embryos were further permeabilized by incubation in proteinase K (5 μg/ml) for 5 minutes, then rinsed in PBS. TdT labeling was followed per manufacturer's

instructions. Anti-DIG-AP (Gibco, 1:100) was used to detect the DIG labeled ends. Brains were flat-mounted in glycerol and imaged.

Inhibition of cell proliferation

Cell proliferation was inhibited by treating embryos with 100 µg/ml aphidicolin (Sigma) in 1% DMSO from 15 hpf until 24 hpf. This treatment significantly slows, although does not stop, cell proliferation. Previous studies have indicated that in zebrafish it is not possible to completely inhibit cell proliferation at the stages observed without severe cell death, which interferes with brain ventricle development (Ikegami et al., 1997). Reduction in cell proliferation was measured using an antibody to phosphorylated histone H3 as described above.

Detection of *snakehead* mutation

Total RNA was extracted from mutant embryos and wild-type siblings using Trizol reagent (Invitrogen), followed by chloroform extraction and isopropanol precipitation. cDNA synthesis was performed with Super Script II Reverse Transcriptase (Invitrogen) and random hexamers. PCR was then performed using five sets of previously published primers, which amplify the coding region of *atp1a1a.1* (Shu et al., 2003). RT-PCR products were used for sequencing analysis, performed by Northwoods DNA, Inc. (Solway MN). Sequencing data was analyzed using the BLAST program (http://www.ncbi.nlm.nih.gov/BLAST/), and the cDNA sequence of *atp1a1a.1* was obtained from the GenBank database (NM_131686). Seven single-nucleotide changes in the *snakehead* cDNA were found, but only one, within primer set 2, changed the amino acid sequence.

Results

Initial opening of zebrafish brain ventricles is rapid

We first characterized brain ventricle formation in wild-type zebrafish embryos using a live imaging method. The hindbrain ventricle was injected with Texas Red conjugated to dextran, which diffused throughout the brain cavities (Fig. 1A), and micrographs taken under light and fluorescent illumination were superimposed (Fig. 1B-K). Using this method, it was apparent that initial ventricle opening was rapid, taking place over a 4-hour period between 18 hpf (Fig. 1B) and 22 hpf (Fig. 1D), during mid-somitogenesis and before the onset of the heartbeat, which begins at 24 hpf (Fig. 1E). Further expansion of the brain ventricles occurred as circulation began (Fig. 1F). Both the midbrain and hindbrain ventricles were shaped by lateral hinge-points, regions of the neuroepithelium that bend sharply (Fig. 1E,J, asterisks). The hindbrain ventricle was the first to open and did so in a diamond-shaped region formed by the pulling apart of two hinge-points, located between the

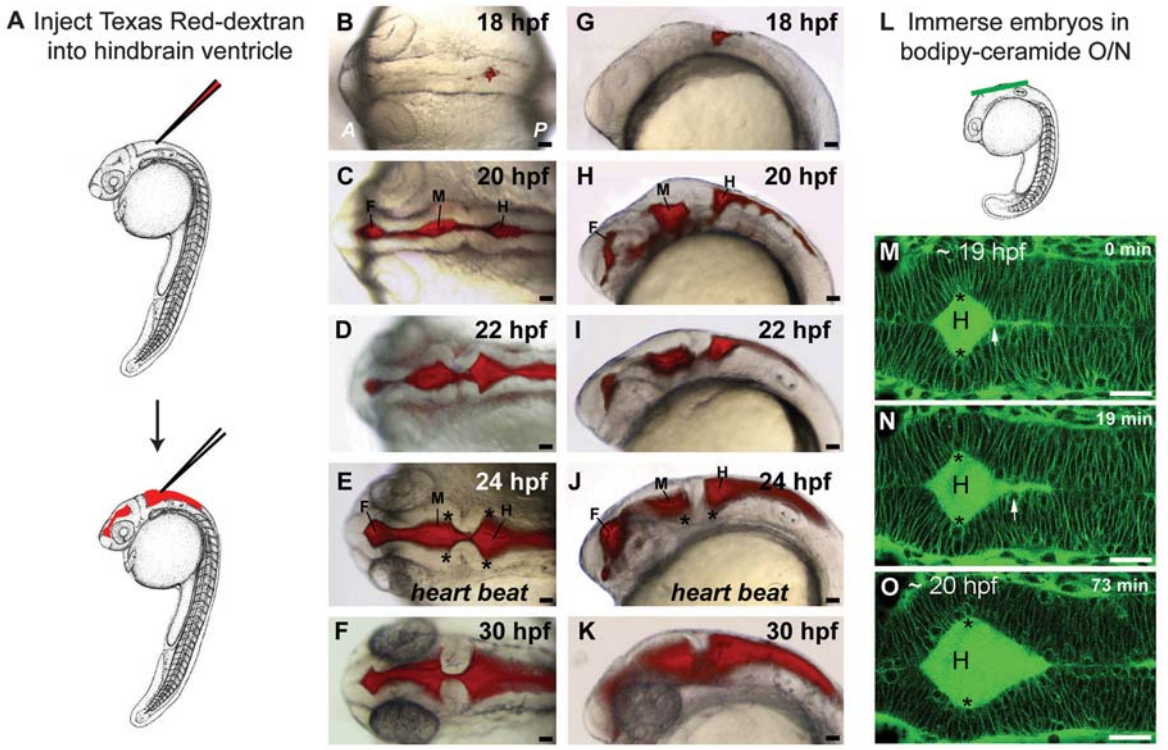

Fig. 1. Timecourse of zebrafish brain ventricle formation. (A-K) Ventricles were visualized by microinjecting a fluorescent dye, Texas Red-dextran, into the hindbrain ventricle of anesthetized embryos. (A) Ventricle injection schematic: lateral view of 24 hpf embryo with microinjection needle at injection site of hindbrain ventricle. (B-K) Developmental profile of brain ventricle morphology at 18, 20, 22, 24, and 30 hpf following dye injection; (B-F) dorsal views; (G-K) lateral views; anterior to left. Heartbeat onset at 24 hpf (E), after brain ventricles have formed. (L-O) Cell morphology of hindbrain ventricle was visualized by confocal microscopy after overnight immersion in fluorescent molecule bodipy ceramide. (L) Diagram of lateral view of 18 hpf embryo, with horizontal plane used for confocal time-lapse imaging indicated by green line. (M-O) Confocal time-lapse imaging of hindbrain ventricle of living, anesthetized embryo, beginning at 19 hpf and ending at 20 hpf. Asterisks label hinge-points from which opening begins, and arrows point to locations of apparent adhesion that release as ventricle opens anterior to posterior. Asterisks: midbrain and hindbrain hinge-points. Scale bar: 50 µm. A, anterior; F, forebrain ventricle; H, hindbrain ventricle; M, midbrain ventricle; P, posterior.

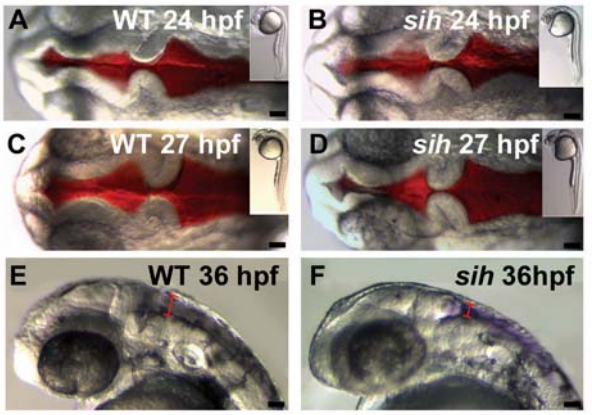

Fig. 2. Initial brain ventricle formation is normal in the absence of circulation. Living, anesthetized embryos from a heterozygous cross of the *silent heart* (*sih*) mutant were injected with Texas Red-dextran. At 24 and 27 hpf, the pattern of ventricle formation is identical in wild type (A,C) and *sih* mutant (B,D). At 36 hpf, the volume of brain ventricles is smaller in *sih* (F) than in wild type (E). (A-D) Dorsal views, (E,F) side views, anterior to left. Scale bar: 50 μm.

upper and lower halves of the rhombic lip (the rhombomere 0 and 1 junction) (Koster and Fraser, 2001; Moens and Prince, 2002) (Fig. 1B-E). Using time-lapse confocal microscopy on living embryos (Fig. 1L-O), we showed that the hindbrain ventricle opened from anterior to posterior, with the apical surfaces of the neuroepithelium pulling apart, to form the ventricular space (Fig. 1M-O) (see Movie 1 in the supplementary material).

These data show that initial brain ventricle formation occurs rapidly, before heartbeat begins, and that the hindbrain ventricle opens in a sequential fashion.

Circulation is not required for initial brain ventricle opening, but is required for later expansion

The demonstration that brain ventricle opening occurred before the onset of heartbeat contrasts with previous speculations that circulation is required for initial brain ventricle development (Schier et al., 1996). In order to further explore this point, we analyzed this process in *silent heart* (*sih*) mutants. The *sih* gene encodes a cardiac-specific troponin, and while the heart forms normally, heartbeat and circulation never occur (Sehnert et al., 2002). *Silent heart* mutants formed brain ventricles indistinguishable from wild type by 24 hpf (Fig. 2A,B). This continued through 27 hpf (Fig. 2C,D). Later during development, by 36 hpf, when wild-type ventricles had expanded their volume significantly (Fig. 2E), *sih* mutants showed a smaller ventricle height (and therefore volume) relative to wild-type embryos (Fig. 2F). These data confirm that initial steps in brain ventricle formation are independent of heartbeat and circulation, but that a later step contributing to ventricle expansion does require circulation. We subsequently focused our attention on the initial opening of the brain ventricles, before 24 hpf.

Requirement for cell proliferation but not cell death in brain ventricle opening

We began to address the mechanism of initial ventricle opening by first asking whether cell proliferation is involved. Whole-

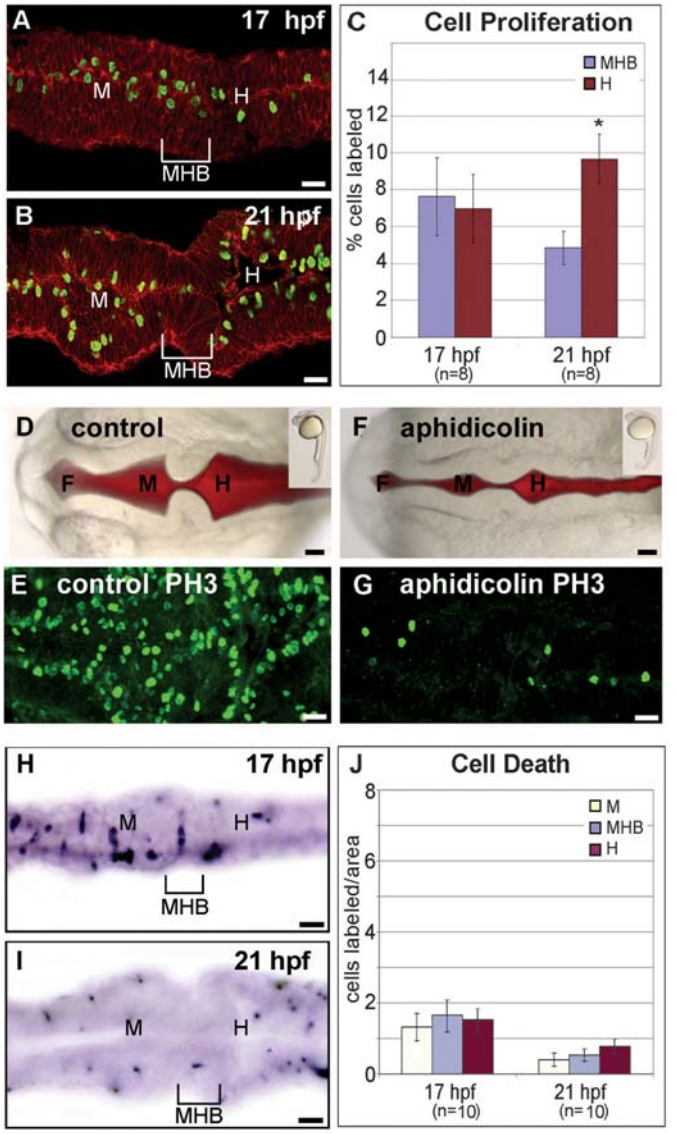

Fig. 3. Cell proliferation and cell death analysis in wild-type and mutant embryos. (A-C) Cell proliferation analysis, using PH3 antibody labeling. (A,B) Fixed and labeled wild-type brain at 17 and 21 hpf. (C) Quantification comparing MHB region and hindbrain, n=8, P=0.627 at 17 hpf; P=0.008 at 21 hpf. Cell proliferation at 21 hpf is significantly higher, showing an almost twofold increase in proliferation in the hindbrain than in the MHB. (D-G) Ventricle formation after inhibition of cell proliferation by aphidicolin treatment. (D,F) Live control and treated embryos after ventricle injection at 24 hpf; (E,G) same embryos as in D and F, fixed and labeled for cell proliferation. Reduced cell proliferation leads to a decrease in ventricle opening. (H-J) Cell death analysis, using TUNEL labeling with ApopTag kit. (H,I) Fixed and labeled wild-type brain at 17 and 21 hpf. (J) Quantification comparing midbrain, MHB and hindbrain regions, n=10, P=0.575 at 17 hpf; P=0.368 at 22 hpf. Error bars denote standard error. H, hindbrain ventricle; M, midbrain ventricle; MHB, midbrain-hindbrain boundary. Scale bar: 50 μm.

mount immunocytochemistry was performed to label mitotic cells with an antibody to phosphorylated histone H3 (PH3) (Hendzel et al., 1997; Saka and Smith, 2001) (Fig. 3A-C). In particular, we asked whether patterns and amounts of cell

Development

division along the anteroposterior (A/P) neuraxis correlated with location of the ventricles. In the straight neural tube, at 17 hpf, before ventricle opening, PH3 labeling was uniform along the A/P axis (Fig. 3A) (n=8, P=0.627). However, by 21 hpf, the number of PH3-positive cells appeared higher in the neural tube surrounding the midbrain and hindbrain ventricles relative to levels in the midbrain-hindbrain boundary (MHB), which does not open to form a ventricle (Fig. 3B). Quantitation of PH3-positive cells showed that at 21 hpf there were approximately twofold more PH3-positive cells in the hindbrain than in the MHB (n=8, P=0.008) (Fig. 3C).

In order to ask whether these different levels of proliferation were significant for ventricle opening, we inhibited cell proliferation by treatment with aphidicolin, which blocks DNA synthesis (Harris and Hartenstein, 1991). Inhibition extended from 15 hpf, before ventricle opening, through 24 hpf, when ventricles would normally have opened (9 hours in total) (Fig. 1). This treatment resulted in reduction of cell proliferation with varying levels (Fig. 3G and data not shown). Reduction in ventricle size was correlated with reduction in cell proliferation (Fig. 3D-G). However, even with extremely reduced levels of PH3 staining, some ventricle opening was observed, and correct ventricle shape and hinge-points were maintained.

We also asked whether cell death was correlated with ventricle opening (Fig. 3H-J). Using TUNEL staining in whole-mount embryos, no patterns of localized cell death were apparent from 17 to 24 hpf (Fig. 3H,I and data not shown). Quantification of cell death demonstrated that, while more death occurred at 17 hpf than at 21 hpf, no brain region examined displayed a significant difference in amount of cell death relative to other regions (Fig. 3J) (n=10, P=0.575 at 17 hpf, P=0.368 at 21 hpf).

These results suggest that regulated cell proliferation is necessary for initial brain ventricle formation, although other processes are crucial. Localized cell death does not appear to regulate initial brain ventricle formation.

The *snakehead* mutant is allelic to *small heart* and corresponds to a point mutation in Na^+K^+ ATPase *atp1a1a.1*

In order to identify brain ventricle mutants, we performed a ‘shelf’ screen of ethylnitrosourea (ENU) and insertional zebrafish mutants (Amsterdam et al., 2004; Jiang et al., 1996; Schier et al., 1996). We focused on mutants that were previously suggested to have a ventricle phenotype, although none of their brain phenotypes have been studied further. From this screen, we have identified 33 mutants with a brain ventricle phenotype, with the important criterion that these show healthy neural tissue, with no obvious necrosis (not shown).

One of the most severe ventricle phenotypes is seen in the *snakehead* (*snk*) mutant. snk^{t0273a} was derived from a large-scale chemical screen and is therefore presumed to be caused by a point mutation (Jiang et al., 1996). In addition to a lack of brain ventricles, *snk* embryos have heart defects, delayed body pigmentation and no touch response (Schier et al., 1996). We noticed that the *snk* phenotype appeared identical to that of the *small heart* (*slh*) mutant, which was isolated in an ENU screen (Yuan and Joseph, 2004). We therefore performed complementation analysis between *snk* and *slh* and determined that they do not complement, and are likely to be different alleles of the same locus. In a cross of *snk* and *slh* heterozygotes, 77% showed a wild-type phenotype and 23% a mutant phenotype (78 embryos in total). *slh* has been cloned and encodes a Na^+K^+ ATPase, Atp1a1a.1 (previously named α1B1). The *heart and mind* (*had*) mutant also has a mutation in the *atp1a1a.1* gene (Shu et al., 2003).

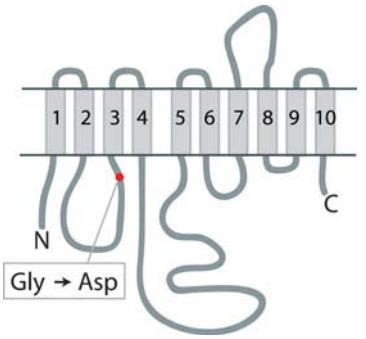

Fig. 4. *snk* encodes the zebrafish Na^+K^+ ATPase Atp1a1a.1 protein. Predicted structure of the Na^+K^+ ATPase Atp1a1a.1 protein. Red dot in the M2-M3 loop represents site of amino acid change from glycine to aspartate at residue 271 in the snk^{to273a} mutant. RT-PCR and sequencing was performed on the *snk* mutants from 3 *snk* carrier clutches (107 embryos), embryos from a *snk* sibling non-carrier clutch (76 embryos) and a wild-type clutch (79 embryos). In 100% of embryos, *snk* mutants, identified phenotypically, showed the G to A mutation, which would result in the glycine to aspartate amino acid change, whereas all wild-type embryos showed the normal G nucleotide.

We asked whether the *snakehead* phenotype was due to a mutation in *atp1a1a.1* by comparing cDNA sequences from the wild-type and $snakehead^{to273a}$ mutants. This analysis revealed that the *to273a* allele of *snakehead* contained a G to A mutation at position 812 in the *atp1a1a.1* coding sequence, which resulted in an amino acid change from glycine to aspartate at position 271 in the amino acid sequence (Fig. 4 and data not shown). This mutation was in the M2-M3 cytoplasmic loop, which is necessary for catalytic activity and may play a role in ion pumping action (Kaplan, 2002). Additional mutations in this loop have been shown to alter the kinetic properties of the protein in other systems (Kaplan, 2002), and thus we predict that the glycine to aspartate mutation in the $snakehead^{to273a}$ mutant substantially reduces or eliminates Na^+K^+ ATPase *atp1a1a.1* function.

It is not clear whether snk^{to273a} is a null mutant. However, *slh* is thought to be a null or severe hypomorph (Yuan and Joseph, 2004), and we are unable to distinguish *snk* and *slh* phenotypes. Further, inhibition of *atp1a1a.1* function by antisense morpholino oligonucleotides does not lead to a more severe phenotype than seen in *snk* or *slh* (Yuan and Joseph, 2004). Together, these data indicate that snk^{to273a} is a null or severe loss-of-function allele of *atp1a1a.1*.

snakehead and *nagie oko* mutants fail to form brain ventricles by different mechanisms

Another mutant with a severe brain ventricle phenotype is *nagie oko* (*nok*), which encodes a MAGUK family kinase required for epithelial cell polarity in the zebrafish eye and gut

(Wei and Malicki, 2002; Horne-Badovinac et al., 2003). We analyzed a retroviral insertion allele of *nagie oko*, isolated in our laboratory, and this hypomorphic allele showed absence of brain ventricles, but did not show the eye phenotype of the ENU-derived *nok* allele, suggesting these may be separable functions, or that there is a quantitatively different requirement for Nok in different tissues (Wei and Malicki, 2002; Wiellette et al., 2004).

By light microscopy of living embryos, brain ventricles appeared completely absent from both mutants in either dorsal views (Fig. 5A-C) or in lateral views (Fig. 5D-F). However, unlike *nok* mutants, the entire *snk* embryo displayed a characteristic refractivity. In particular, in dorsal view, the outline of the neural tube was not visible, even though a neural tube was present (see below). The refractivity of the neural tube thus could not be distinguished from that of surrounding tissues, unlike the case in wild-type embryos. In order to ask whether absence of ventricles in both mutants reflected disruption of a similar process, we further analyzed the brain morphology of the mutants.

Transverse sections of fixed embryos showed that the phenotypes of *snk* and *nok* were strikingly distinct (Fig. 5G-O). In wild-type embryos at 22 hpf, different regions of the brain showed characteristic brain ventricle morphology. The forebrain ventricle opened into a diamond shape (Fig. 5G) and the midbrain ventricle showed a cruciform morphology with lateral and dorsoventral hinge-points (Fig. 5J, asterisks), while the hindbrain ventricle showed lateral hinge-points as well as a very thin dorsal epithelial covering (Fig. 5M). Sections of *snk* showed that these morphologies were present in *snk* embryos (Fig. 5H,K,N); however, there were no visible extracellular spaces, all cells seemed stuck together, and the lumen never opened. Normal morphogenesis was most clearly visible in the *snk* midbrain, which showed the wild-type cruciform shape (Fig. 5K), and hindbrain, which had a thin covering sheet (Fig. 5N). By contrast, the *nok* mutant neural tube remained uniform

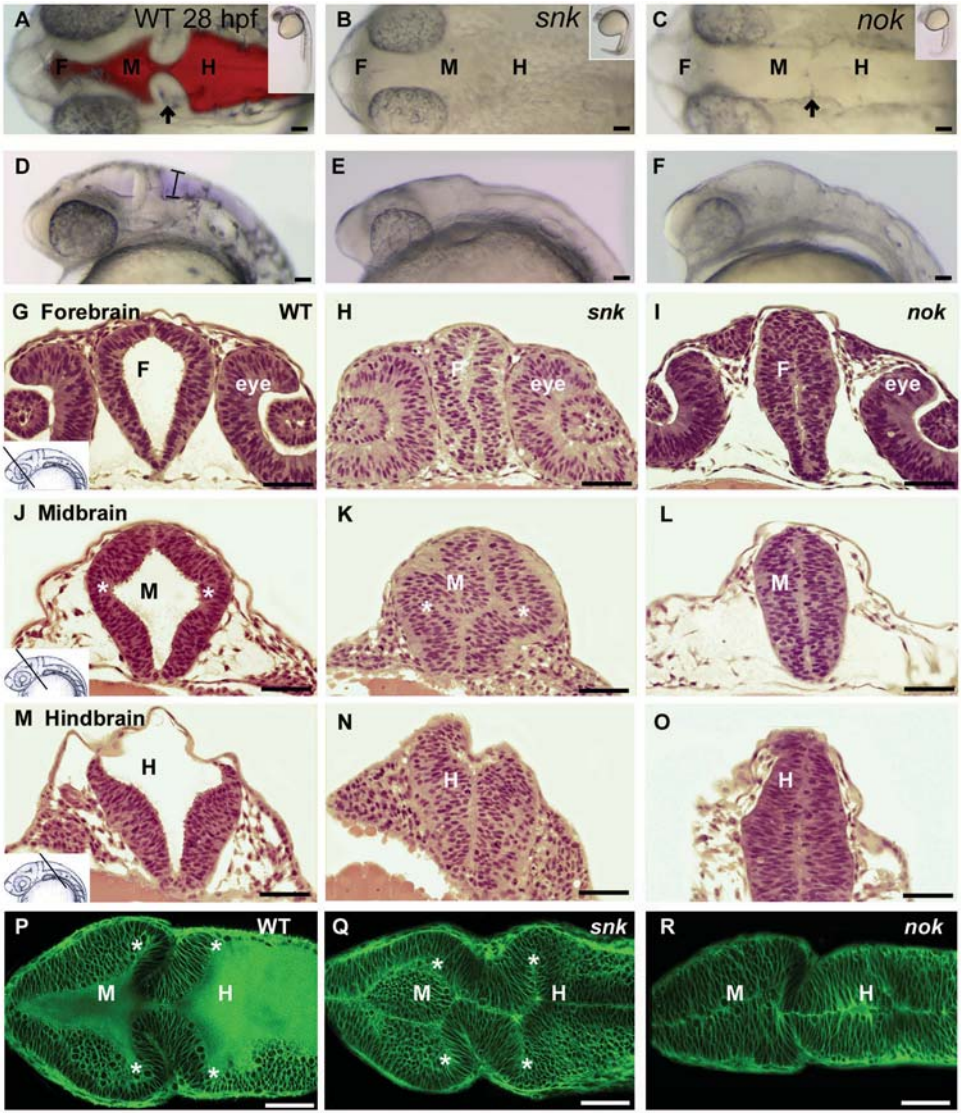

Fig. 5. Morphological analysis of *snakehead* and *nagie oko* brain ventricle mutants. (A-F) Light microscopy images of brain at 28 hpf. Dorsal views (A-C) or side views (D-F) of living, anesthetized embryos are shown, anterior to left. Ventricles are injected with Texas Red dextran in A. Relative to wild-type (A,D), brain ventricles in *snakehead* (B,E) and *nagie oko* (C,F) mutants appear to be absent: *nok* mutants sometimes form a small hindbrain ventricle that never enlarges. Note the characteristic refractivity of the neural tube in *snk*, in that neither the outline of the neural tube nor the brain folds are visible in the *snk* mutant (B,E). In addition, note that arrows in A and C point to the MHB constriction in wild type and *nok*, respectively. By light microscopy, the *snk* MHB constriction is not visible (even though it is in the proper location; see Q below). Bracket in D indicates hindbrain ventricle height. (G-O) Histology of *snk* and *nok* mutants. Embryos were fixed and transverse-sectioned at 22 hpf, at the level of forebrain, midbrain or hindbrain, and stained with hematoxylin and eosin. Relative to wild-type embryos (G,J,M), *snk* mutant embryos (H,K,N) show appropriate ventricle morphology; however, the cells appear to be adhered to one another and no lumen is present. By contrast, *nok* mutant embryos (I,L,O) fail to undergo any ventricle morphogenesis, and the epithelium appears disorganized. Asterisks label midbrain hinge-points in wild type (J) and *snk* (K), but hinge-points are absent in *nok* (L). (P-R) Confocal images through mid- and hindbrain ventricles of 24 hpf living embryos stained with bodipy ceramide. (P) Wild type, (Q) *snk*, (R) *nok*. Note that *snk* embryos (Q) assume correct ventricle morphology but fail to open the ventricles. By contrast, the brain tube in *nok* embryos (R) remains straight and no hinge-points form (although the MHB constriction remains). Scale bar: 50 μm. F, forebrain ventricle; H, hindbrain ventricle; M, midbrain ventricle. Asterisks: hinge-points.

Development

in transverse section, with no lateral hinge-points (Fig. 5I,L,O), resembling the 17 hpf neural tube before ventricle morphogenesis (not shown). In some *nok* embryos, the dorsal neural tube did appear thinner in the hindbrain region (not shown), indicating that this aspect of brain morphogenesis was normal. Confocal microscopy of living embryos confirmed the different phenotypes of these two mutants (Fig. 5P-R). Thus, while *snk* brain morphology appeared normal except for the lack of brain ventricle inflation (Fig. 5Q), the *nok* neuroepithelium failed to undergo morphogenesis, with no midbrain or hindbrain lateral hinge-points (Fig. 5R).

These data show that both *snk* and *nok* have an early ventricle phenotype, by 20 hpf, before the onset of heartbeat. Significantly, the 'no ventricle' phenotypes of *snk* and *nok* mutants were quite different, which indicates that the mechanisms by which these genes affect brain ventricle morphogenesis are distinct.

nagie oko mutants retain epithelial polarity but lose epithelial integrity in the brain

Previous analyses of *nok* mutants have concluded that, within the brain, epithelial polarity is normal, whereas in the retina, epithelial polarity is abnormal and correlated with retinal disorganization (Wei and Malicki, 2002). However, the brain epithelium has not been extensively examined, and we therefore analyzed *nok* epithelial organization in more detail. We first examined transverse brain sections at 17 hpf, when the neural tube is normally straight and ventricle morphogenesis has not yet begun. Sections of wild-type embryos showed a clear midline, with nuclei lined up on either side (Fig. 6A), while *nok* mutant sections showed disorganized nuclear position and no continuous midline (Fig. 6B). However, in most sections of *nok* mutants extending from forebrain to hindbrain, there were small, intermittent regions with a clear midline (not shown).

As epithelial polarity and junctions have not been thoroughly examined in the *nok* brain epithelium, we analyzed expression of various junction and cell polarity markers in *nok* mutants using immunohistochemistry. As indicators of adherens junctions, β-catenin and actin expression were analyzed, while occludin expression was used as a tight junction marker (Furuse et al., 1993; Nagafuchi, 2001), all of which are normally found at the apical side of tightly connected cells of an epithelium. In *nok* mutants, β-catenin, actin and occludin proteins were localized apically, and no ectopic foci were observed at other regions of the cell membrane, indicating correct apical/basal polarity was present (Fig. 6C-L). However, consistent with histological sections, labeling did not occur along a distinct brain midline, and instead there were regions where labeling was missing (compare Fig. 6E and F, 6G and H, 6I and J). This was particularly apparent when observing actin foci at high magnification (Fig. 6K,L). In a three-dimensional confocal image of the labeled wild-type brain, an actin belt surrounding the apicolateral surface of each cell in the epithelium was visible (Fig. 6K). However, this belt was not present in *nok* mutants and instead the actin foci were disorganized (Fig. 6L). As a further test for correct apical/basal polarity, we also asked about our *nok* hypomorphic allele whether residual Nok protein was correctly localized, using an antibody to Nok (Wei and Malicki, 2002). A small amount of protein was correctly localized in the *nok* mutant (Fig. 6N); however, this appeared much reduced compared with wild type (Fig. 6M).

In summary, we showed that in the future brain the *nok* neuroepithelium was highly disorganized, and that while it displayed proper apical/basal organization, junctional actin belts did not form cohesively, and there was no clear or continuous midline.

Epistasis analysis of *snakehead/atp1a1a.1* and *nagie oko*

As both *snk* and *nok* mutants fail to form ventricles, we performed epistasis analysis to determine whether the *atp1a1a.1* and *nok* genes function in the same or separate genetic pathways (Fig. 7). To create double-mutant embryos, heterozygote carriers were mated and their progeny raised. Double mutants were identified by morphology and PCR.

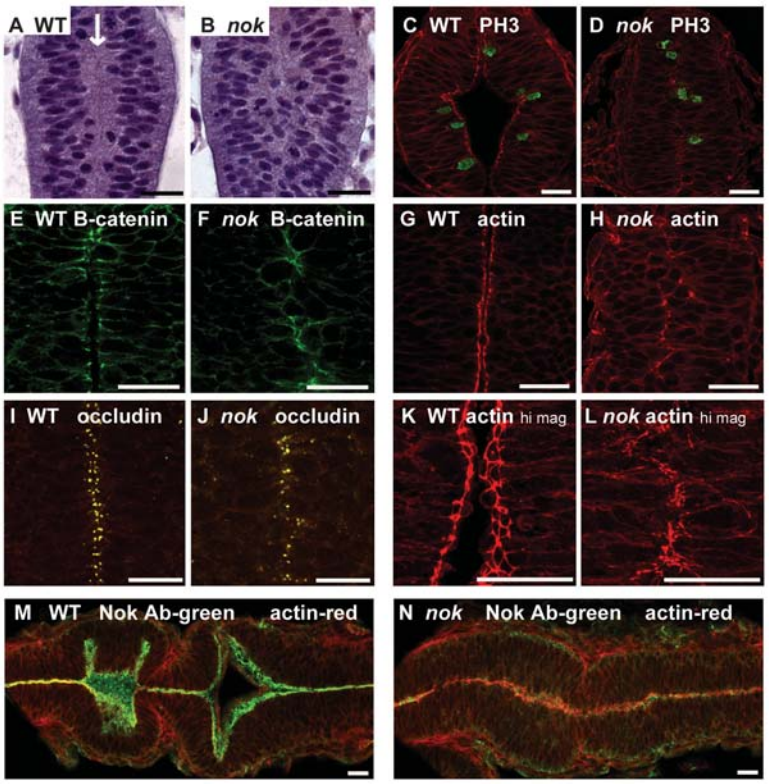

Fig. 6. Analysis of epithelial integrity in *nok* mutants. (A-L) Transverse sections through brains of wild-type and *nok* embryos at 17 hpf (A,B) or 22 hpf (C-L). (A,B) A clear midline is visible in wild type (A; arrow) but cells are disorganized in *nok* (B). (C,D) Labeled with PH3 antibody (mitosis marker) (green) and actin (red), dividing nuclei localize apically in both wild type (C) and mutant (D). (E,F) Labeled with β-catenin antibody; (G,H) labeled with actin marker, phalloidin-Texas Red; (I,J) labeled with occludin antibody and phalloidin-Texas Red counterstain; (K,L) high magnification of 3D compilation of transverse sections through forebrain, labeled with phalloidin-Texas Red. In the *nok* mutant, all junction markers localize apically as in wild type but show disorganization. (M,N) Nok antibody labeling (green) at 22 hpf in horizontal section through midbrain and hindbrain of wild type (M) and *nok* mutant (N), with phalloidin-Texas Red as counterstain (red). Scale bar: 20 μm.

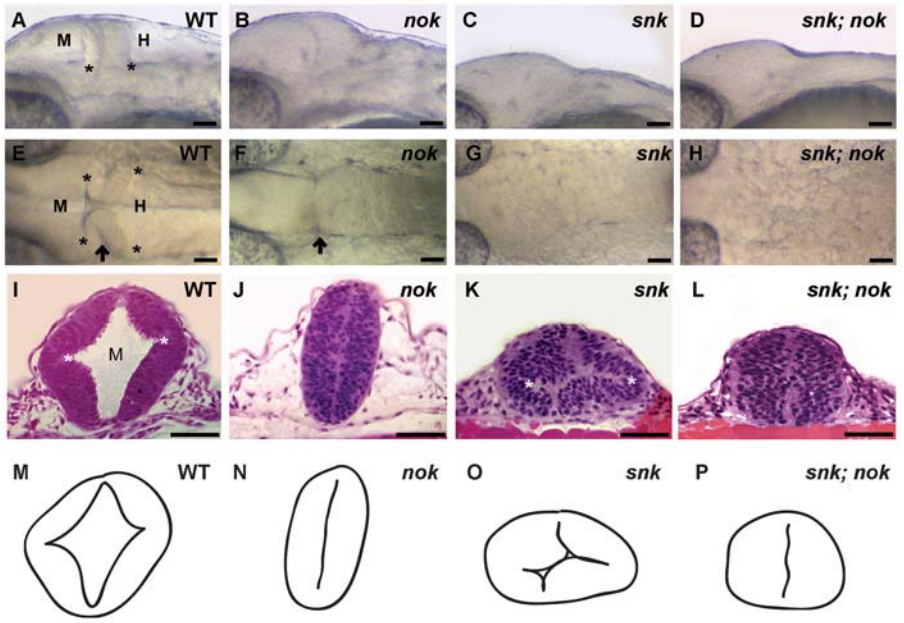

Fig. 7. Epistasis analysis of brain ventricle mutants *snk* and *nok*. (A-H) Lateral and dorsal views of anesthetized, living embryos at 25 hpf. (A,E) Wild type (70/139 embryos, 50%); (B,F) *nagie oko* mutants (29/139 embryos, 21%); (C,G) *snakehead* mutants (30/139 embryos, 22%). (D,H) *snakehead;nagie oko* double mutants (10/139, 7%) show overall composite phenotype. Asterisks mark hinge-points, which are visible in wild type but not visible in the mutants (although hinge-points are present in the *snk* mutant; see K). Arrow marks midbrain-hindbrain constriction, which is visible in wild type and *nok* mutant but is not visible in *snk* nor *snk;nok* due to the altered refractivity of the *snk* tissue. (I-L) Histological sections through midbrain at 22 hpf of wild type (I), *nok* (J), *snk* (K) and *snk;nok* (L). The phenotype appears to be additive, suggesting *nagie oko* and *snakehead* function in separate pathways. (M-P) Drawings of brain outline and ventricle lumen in I-L show composite phenotype more clearly. Scale bar: 50 μm. H, hindbrain ventricle; M, midbrain ventricle.

Light microscopy and histology showed that the double mutant *snk;nok* had a composite of both mutant phenotypes (Fig. 7D,H,L,P). In the double mutant, the altered refractivity and lack of extracellular spaces of the *snk* phenotype was present (Fig. 7C,G,K,O). However, the narrower brain tube, disorganized epithelium, and lack of hinge-points characteristic of the *nok* phenotype was also present (Fig. 7B,F,J,N and Fig. 7D,H,L,P).

We wondered whether the *nok*-like ventricle morphology indicated that *nok* is required to activate *atp1a1a.1* function. In order to address this, we asked whether Atp1a1a.1 was correctly localized in *nok* mutants (Fig. 8A,B). An antibody (a6F) that recognizes multiple Na^+K^+ATPases was used (Drummond et al., 1998; Takeyasu et al., 1988) as Atp1a1a.1-specific antibodies are not yet available. In both wild-type and *nok* embryos, a6F antibody staining was present at the apical surface of the neuroepithelium, whether or not the ventricle had opened (Fig. 8A,B).

In addition, we assayed Nok localization in the *snk* mutant. In both wild-type and *snk* embryos, Nok antibody staining was localized apically (Fig. 8C,D), suggesting that Atp1a1a.1 function is not necessary for correct targeting of Nok to the apical membrane. Moreover, actin-associated adherens junctions were intact in the *snk* mutant, as shown by phalloidin-Texas Red labeling (data not shown), further substantiating that Atp1a1a.1 is not affecting epithelial integrity.

In summary, the composite double-mutant phenotype and correct localization of a6F staining and Nok protein in *nok* and *snk* mutants, respectively, suggest that *nagie oko* and *atp1a1a.1* function in separate pathways.

Discussion

Multiple steps are required for brain ventricle development

Brain ventricle formation is one of the earliest manifestations of three-dimensional brain structure. Using the zebrafish as a model, we can distinguish several steps required for ventricle development (Fig. 9). Three early steps occur rapidly, over a 4 hour period, and are circulation-independent. One step leads to morphogenesis of the closed neural tube and to formation of lateral hinge-points at specific A/P positions. Morphogenesis requires an intact, polarized epithelium and is dependent on Nagie oko protein function. A second step is inflation of the ventricle lumen that requires activity of the Atp1a1a.1 ion pump, and presumably subsequent osmosis to open the ventricular spaces. Regulated cell proliferation appears to be a third input into ventricle development. A later process of ventricle expansion occurs after circulation has begun, and is circulation-dependent.

Two distinct periods during initiation and expansion of brain ventricles: the role of circulation

Most zebrafish mutants that show brain ventricle defects also display heart or circulation defects (Schier et al., 1996). Previous studies have shown that circulation is necessary for maintenance of brain ventricle size in adult animals, and that reduction in blood pressure leads to reduction in CSF secretion and pressure within the ventricles (Deane and Segal, 1979). It was therefore suggested that zebrafish brain ventricle defects developed secondarily to the circulation defect (Schier et al., 1996). This reasoning also stemmed from studies in chick, which showed that after the onset of circulation a positive CSF pressure inside the brain ventricles is necessary for brain ventricle expansion (Desmond, 1985; Desmond and Jacobson, 1977; Desmond and Levitan, 2002).

Our data show that initial stages of ventricle formation are not dependent on circulation. Why do many mutants with brain ventricle defects also display heart or circulation defects? One possibility is that some of these mutants show a ‘late’ ventricle phenotype and reflect a deficit in circulation-dependent ventricle expansion. Another possibility is that genes required for heart and brain ventricle morphogenesis are shared and the phenotype of a particular mutant is therefore pleiotropic. In support of this, both *nagie oko* and *snakehead* mutants show heart defects.

Development

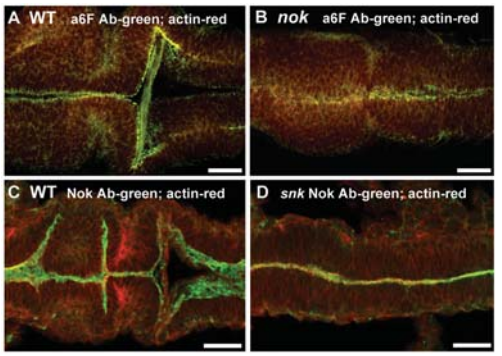

Fig. 8. α-Na^+K^+ ATPase localization in *nok* mutants and Nok localization in *snk* mutants appears normal. (A,B) a6F antibody labeling (green) at 24 hpf in horizontal section through midbrain and hindbrain of wild type (A) and *nok* mutant (B) with phalloidin-Texas Red as counterstain (red). Note that while the *nok* mutant hindbrain ventricle is severely reduced, a6F antibody still labels apical membrane. (C,D) Nok antibody labeling (green) at 24 hpf in horizontal section through midbrain and hindbrain of wild type (C) and *snk* mutant (D), with phalloidin-Texas Red as counterstain (red). Nok localizes at the apical membrane in both wild type (C) and mutant (D), suggesting that Snk is not necessary for Nok targeting to apical surface. Note: the *snk* mutant does have normal hinge-points in the midbrain and hindbrain, although they are not present in the optical section shown in D. Scale bar: 50 μm.

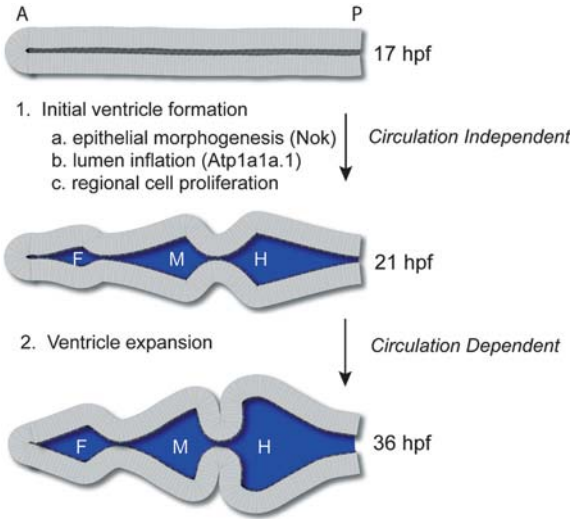

Fig. 9. Multiple steps are required for brain ventricle formation. Three steps have been identified during initial brain ventricle formation and occur independently of circulation. The Nagie oko protein helps maintain epithelial polarity and/or integrity, which is required for normal ventricle morphogenesis. Atp1a1a.1 is essential to inflate the ventricular space with fluid, and localized cell proliferation also appears to be necessary. Later brain ventricle expansion requires circulation. A, anterior; F, forebrain ventricle; H, hindbrain ventricle; M, midbrain ventricle; P, posterior.

The role of cell proliferation in brain ventricle development

The lowest level of cell proliferation we observed along the A/P axis of the brain epithelium was at the MHB, and this deficit may be one of the reasons that the MHB does not open into a ventricular space. How might cell proliferation contribute to normal ventricle development? One possibility is that a critical mass of cells is necessary for ventricle morphogenesis, while a second is that cells must be actively cycling to respond to signals leading to cell movement or shape changes. A third possibility is that cell proliferation is required for lumen inflation, rather than for ventricle morphogenesis. However, the smaller, but normally shaped, ventricles observed after inhibition of DNA replication did not resemble the defects seen in *nok* or *snk* mutants, and neither of these mutants showed differences in cell proliferation (or cell death) relative to wild-type embryos (not shown). We therefore hypothesize that cell proliferation defines an independent step during ventricle formation. We cannot rule out that embryos in which cell proliferation had been inhibited were generally disrupted; however, other regions of such embryos appeared normal, including somite number and shape (not shown). Overproliferation of the neuroepithelium also suppresses ventricle opening, as shown in the *mindbomb* and *curlyfry* mutants (Bingham et al., 2003; Song et al., 2004), and the connection between these data and the requirement for cell proliferation is not clear.

Previous reports have indicated that in mice blocking cell death by caspase gene ablation causes an overgrowth of the brain tissue, with obscured or obstructed brain ventricles (Kuida et al., 1996). Conversely, mutations that cause too much cell death in the brain lead to a reduction in brain tissue and overexpansion of the brain ventricles (Keino et al., 1994). Our data do not suggest an early role for regulated cell death in initial brain ventricle development, and it is likely that these phenotypes reflect late outcomes of perturbing cell death.

The *nagie oko* phenotype indicates a requirement for epithelial integrity in ventricle formation

The *nagie oko* gene encodes a MAGUK family scaffolding protein that localizes to junctions at the apical surface of epithelia and regulates epithelial polarity (Wei and Malicki, 2002). MAGUK proteins probably function in the assembly of protein complexes that control the formation or maintenance of cell junctions, and the Nok homolog in other organisms (*Stardust* in *Drosophila*, PALS1 in mammals) is part of the Crumbs protein complex, one of the key regulators of epithelial junction formation (Bachmann et al., 2001; Hong et al., 2001; Hurd et al., 2003; Knust and Bossinger, 2002; Muller and Bossinger, 2003; Tepass, 2002).

Brain ventricle morphogenesis may require a cohesive epithelium, and *nok* mutants may fail to undergo morphogenesis because the brain neuroepithelium lacks normal epithelial junctions and therefore lacks this cohesiveness. Additionally, in *nok* mutants, there is no continuous midline, at which opposing epithelial surfaces would normally separate. The *nok* phenotype may therefore arise because the neuroepithelium is glued shut by cells straddling the midline. In support of this, *nok* mutants often show short stretches of a clear midline, and perhaps correlated with this, sometimes show very small ventricular openings.

Atp1a1a.1 plays a role in lumen inflation

The mechanism by which the brain ventricles initially inflate

is not known. The Na^+K^+ ATPase Atp1a1a.1 protein is likely to be necessary to create an osmotic gradient that would drive movement of water into the closed ventricles after their morphogenesis (Blanco and Mercer, 1998; Speake et al., 2001; Therien and Blostein, 2000). We therefore hypothesize that Atp1a1a.1 functions to direct initial brain ventricle lumen inflation. The sequential opening of each ventricle may reflect sequential activation of this ion pump, thus blowing up the ventricles like a balloon. Alternately, Atp1a1a.1 function may be continuous along the length of the brain, and another mechanism may regulate where initial lumen inflation occurs. Interestingly, although the Na^+K^+ ATPase family is large, other members cannot compensate for the loss of embryonic Atp1a1a.1 function. This is consistent with previous results showing that similar alpha subunits of Na^+K^+ ATPase do not show the same expression patterns and cannot substitute for each other during zebrafish heart development or ear development (Canfield et al., 2002; Shu et al., 2003; Blasiole et al., 2003).

In the older brain, the choroid plexuses are the main source of CSF secretion, although the brain ependymal cells also contribute (Wright, 1978; Brown et al., 2004; Bruni, 1998). Na^+K^+ ATPases localize to the ventricular surface of secretory brain epithelia in adult mammals and amphibia and are necessary for the secretion of CSF (Masuzawa et al., 1984; Saito and Wright, 1983). Thus, this gene family may be used at different times of development to initiate, and later maintain, ventricular fluid secretion. We hypothesize that earlier during development, when the brain ventricles are initially forming and before the choroid plexuses have formed, the ependymal cells lining the ventricles are the source of CSF, through the action of the Atp1a1a.1 protein.

Zebrafish as a model for vertebrate brain ventricle development

In some respects, formation of the zebrafish neural tube appears different from that of frog, as in the brain region the zebrafish neural tube is initially straight whereas in the frog *Xenopus* the presumptive brain undergoes some morphogenesis prior to neural tube closure. However, the number, position and shape of the initial brain ventricles are essentially identical in all vertebrates. We have previously compared processes of trunk neural tube formation between teleosts and other vertebrates, and have concluded that these are very similar (Lowery and Sive, 2004) (see Introduction). These considerations suggest that zebrafish ventricle formation is likely to be fundamentally the same as that of other vertebrates. We are beginning to analyze the phenotypes of other zebrafish ventricle mutants, and this is likely to uncover additional genetic mechanisms regulating brain ventricle formation. Of particular interest is the relationship between genes that regulate neural patterning and the positioning and shaping of the ventricles, the interaction of *nok* with other genes that regulate epithelial polarity, and the mechanism by which *atp1a1a.1* and other genes regulate lumen inflation.

We thank members of the Sive lab for helpful comments and Ben Pratt for fish husbandry. Many thanks to Randall Peterson for clutches of *silent heart* mutant embryos, Shipeng Yuan and Calum Macrae for providing unpublished information related to the *small heart* mutation, the Nusslein-Volhard lab for providing us with the *snakehead* mutant, Jarema Malicki and Xiangyun Wei for *nok* morpholino sequence, Nok antibody and *nok*^{m227}, Ryan Murphy (Zon lab) for information on blocking cell proliferation, and Jaunian Chen for helpful discussions. This work was conducted utilizing the W. M. Keck Foundation Biological Imaging Facility at the Whitehead Institute. Supported by NIH MH70926 and MH59942 to H.L.S. L.A.L. is the recipient of the Abraham J. Siegel Fellowship at the Whitehead Institute.

Supplementary material

Supplementary material for this article is available at
http://dev.biologists.org/cgi/content/full/132/9/2057/DC1

References

Alonso, M. I., Gato, A., Moro, J. A. and Barbosa, E. (1998). Disruption of proteoglycans in neural tube fluid by beta-D-xyloside alters brain enlargement in chick embryos. *Anat. Rec.* **252**, 499-508.

Alonso, M. I., Gato, A., Moro, J. A., Martin, P. and Barbosa, E. (1999). Involvement of sulfated proteoglycans in embryonic brain expansion at earliest stages of development in rat embryos. *Cells Tissues Organs* **165**, 1-9.

Amsterdam, A., Nissen, R. M., Sun, Z., Swindell, E. C., Farrington, S. and Hopkins, N. (2004). Identification of 315 genes essential for early zebrafish development. *Proc. Natl. Acad. Sci. USA* **101**, 12792-12797.

Bachmann, A., Schneider, M., Theilenberg, E., Grawe, F. and Knust, E. (2001). Drosophila Stardust is a partner of Crumbs in the control of epithelial cell polarity. *Nature* **414**, 638-643.

Bingham, S., Chaudhari, S., Vanderlaan, G., Itoh, M., Chitnis, A. and Chandrasekhar, A. (2003). Neurogenic phenotype of mind bomb mutants leads to severe patterning defects in the zebrafish hindbrain. *Dev. Dyn.* **228**, 451-463.

Blanco, G. and Mercer, R. W. (1998). Isozymes of the Na-K-ATPase: heterogeneity in structure, diversity in function. *Am. J. Physiol.* **275**, F633-650.

Blasiole, B., Degrave, A., Canfield, V., Boehmler, W., Thisse, C., Thisse, B., Mohideen, M. A. and Levenson, R. (2003). Differential expression of Na,K-ATPase alpha and beta subunit genes in the developing zebrafish inner ear. *Dev. Dyn.* **228**, 386-392.

Brown, P. D., Davies, S. L., Speake, T. and Millar, I. D. (2004). Molecular mechanisms of cerebrospinal fluid production. *Neuroscience* **129**, 955-968.

Bruni, J. E. (1998). Ependymal development, proliferation, and functions: a review. *Microsc. Res. Tech.* **41**, 2-13.

Canfield, V. A., Loppin, B., Thisse, B., Thisse, C., Postlethwait, J. H., Mohideen, M. A., Rajarao, S. J. and Levenson, R. (2002). Na,K-ATPase alpha and beta subunit genes exhibit unique expression patterns during zebrafish embryogenesis. *Mech. Dev.* **116**, 51-59.

Cooper, M. S., D'Amico, L. A. and Henry, C. A. (1999). Confocal microscopic analysis of morphogenetic movements. *Methods Cell Biol.* **59**, 179-204.

Cushing, H. (1914). Studies on the cerebrospinal fluid. I. Introduction. *J. Med. Res.* **26**, 1-19.

Deane, R. and Segal, M. B. (1979). The effect of vascular perfusion of the choroid plexus on the secretion of cerebrospinal fluid [proceedings]. *J. Physiol.* **293**, 18P-19P.

Dent, J. A., Polson, A. G. and Klymkowsky, M. W. (1989). A whole-mount immunocytochemical analysis of the expression of the intermediate filament protein vimentin in Xenopus. *Development* **105**, 61-74.

Desmond, M. E. (1985). Reduced number of brain cells in so-called neural overgrowth. *Anat. Rec.* **212**, 195-198.

Desmond, M. E. and Jacobson, A. G. (1977). Embryonic brain enlargement requires cerebrospinal fluid pressure. *Dev. Biol.* **57**, 188-198.

Desmond, M. E. and Levitan, M. L. (2002). Brain expansion in the chick embryo initiated by experimentally produced occlusion of the spinal neurocoel. *Anat. Rec.* **268**, 147-159.

Drummond, I. A., Majumdar, A., Hentschel, H., Elger, M., Solnica-Krezel, L., Schier, A. F., Neuhauss, S. C., Stemple, D. L., Zwartkruis, F., Rangini, Z. et al. (1998). Early development of the zebrafish pronephros and analysis of mutations affecting pronephric function. *Development* **125**, 4655-4667.

Furuse, M., Hirase, T., Itoh, M., Nagafuchi, A., Yonemura, S. and Tsukita,

S. (1993). Occludin: a novel integral membrane protein localizing at tight junctions. *J. Cell Biol.* **123**, 1777-1788.
Guo, S., Wilson, S. W., Cooke, S., Chitnis, A. B., Driever, W. and Rosenthal, A. (1999). Mutations in the zebrafish unmask shared regulatory pathways controlling the development of catecholaminergic neurons. *Dev. Biol.* **208**, 473-487.
Hardan, A. Y., Minshew, N. J., Mallikarjuhn, M. and Keshavan, M. S. (2001). Brain volume in autism. *J. Child Neurol.* **16**, 421-424.
Harris, W. A. and Hartenstein, V. (1991). Neuronal determination without cell division in Xenopus embryos. *Neuron* **6**, 499-515.
Hendzel, M. J., Wei, Y., Mancini, M. A., Van Hooser, A., Ranalli, T., Brinkley, B. R., Bazett-Jones, D. P. and Allis, C. D. (1997). Mitosis-specific phosphorylation of histone H3 initiates primarily within pericentromeric heterochromatin during G2 and spreads in an ordered fashion coincident with mitotic chromosome condensation. *Chromosoma* **106**, 348-360.
Hong, Y., Stronach, B., Perrimon, N., Jan, L. Y. and Jan, Y. N. (2001). Drosophila Stardust interacts with Crumbs to control polarity of epithelia but not neuroblasts. *Nature* **414**, 634-638.
Horne-Badovinac, S., Rebagliati, M. and Stainier, D. Y. (2003). A cellular framework for gut-looping morphogenesis in zebrafish. *Science* **302**, 662-665.
Hurd, T. W., Gao, L., Roh, M. H., Macara, I. G. and Margolis, B. (2003). Direct interaction of two polarity complexes implicated in epithelial tight junction assembly. *Nat. Cell Biol.* **5**, 137-142.
Ikegami, R., Rivera-Bennetts, A. K., Brooker, D. L. and Yager, T. D. (1997). Effect of inhibitors of DNA replication on early zebrafish embryos: evidence for coordinate activation of multiple intrinsic cell-cycle checkpoints at the mid-blastula transition. *Zygote* **5**, 153-175.
Jiang, Y. J., Brand, M., Heisenberg, C. P., Beuchle, D., Furutani-Seiki, M., Kelsh, R. N., Warga, R. M., Granato, M., Haffter, P., Hammerschmidt, M. et al. (1996). Mutations affecting neurogenesis and brain morphology in the zebrafish, Danio rerio. *Development* **123**, 205-216.
Kaplan, J. H. (2002). Biochemistry of Na,K-ATPase. *Annu. Rev. Biochem.* **71**, 511-535.
Keino, H., Masaki, S., Kawarada, Y. and Naruse, I. (1994). Apoptotic degeneration in the arhinencephalic brain of the mouse mutant Pdn/Pdn. *Brain Res. Dev. Brain Res.* **78**, 161-168.
Kimmel, C. B., Ballard, W. W., Kimmel, S. R., Ullmann, B. and Schilling, T. F. (1995). Stages of embryonic development of the zebrafish. *Dev. Dyn.* **203**, 253-310.
Knust, E. and Bossinger, O. (2002). Composition and formation of intercellular junctions in epithelial cells. *Science* **298**, 1955-1959.
Koster, R. W. and Fraser, S. E. (2001). Direct imaging of in vivo neuronal migration in the developing cerebellum. *Curr. Biol.* **11**, 1858-1863.
Kuida, K., Zheng, T. S., Na, S., Kuan, C., Yang, D., Karasuyama, H., Rakic, P. and Flavell, R. A. (1996). Decreased apoptosis in the brain and premature lethality in CPP32-deficient mice. *Nature* **384**, 368-372.
Kurokawa, K., Nakamura, K., Sumiyoshi, T., Hagino, H., Yotsutsuji, T., Yamashita, I., Suzuki, M., Matsui, M. and Kurachi, M. (2000). Ventricular enlargement in schizophrenia spectrum patients with prodromal symptoms of obsessive-compulsive disorder. *Psychiatry Res.* **99**, 83-91.
Lowery, L. A. and Sive, H. (2004). Strategies of vertebrate neurulation and a re-evaluation of teleost neural tube formation. *Mech. Dev.* **121**, 1189-1197.
Masuzawa, T., Ohta, T., Kawamura, M., Nakahara, N. and Sato, F. (1984). Immunohistochemical localization of Na+, K+-ATPase in the choroid plexus. *Brain Res.* **302**, 357-362.
McAllister, J. P., 2nd and Chovan, P. (1998). Neonatal hydrocephalus. Mechanisms and consequences. *Neurosurg. Clin. N. Am.* **9**, 73-93.
Milhorat, T. H., Hammock, M. K., Fenstermacher, J. D. and Levin, V. A. (1971). Cerebrospinal fluid production by the choroid plexus and brain. *Science* **173**, 330-332.
Miyan, J. A., Nabiyouni, M. and Zendah, M. (2003). Development of the brain: a vital role for cerebrospinal fluid. *Can. J. Physiol. Pharmacol.* **81**, 317-328.
Moens, C. B. and Prince, V. E. (2002). Constructing the hindbrain: insights from the zebrafish. *Dev. Dyn.* **224**, 1-17.
Muller, H. A. and Bossinger, O. (2003). Molecular networks controlling epithelial cell polarity in development. *Mech. Dev.* **120**, 1231-1256.
Nagafuchi, A. (2001). Molecular architecture of adherens junctions. *Curr. Opin. Cell Biol.* **13**, 600-603.
Novak, Z., Krupa, P., Zlatos, J. and Nadvornik, P. (2000). The function of the cerebrospinal fluid space and its expansion. *Bratisl. Lek. Listy* **101**, 594-597.
Owen-Lynch, P. J., Draper, C. E., Mashayekhi, F., Bannister, C. M. and Miyan, J. A. (2003). Defective cell cycle control underlies abnormal cortical development in the hydrocephalic Texas rat. *Brain* **126**, 623-631.
Pollay, M. and Curl, F. (1967). Secretion of cerebrospinal fluid by the ventricular ependyma of the rabbit. *Am. J. Physiol.* **213**, 1031-1038.
Rekate, H. L. (1997). Recent advances in the understanding and treatment of hydrocephalus. *Semin. Pediatr. Neurol.* **4**, 167-178.
Saito, Y. and Wright, E. M. (1983). Bicarbonate transport across the frog choroid plexus and its control by cyclic nucleotides. *J. Physiol.* **336**, 635-648.
Saka, Y. and Smith, J. C. (2001). Spatial and temporal patterns of cell division during early Xenopus embryogenesis. *Dev. Biol.* **229**, 307-318.
Schier, A. F., Neuhauss, S. C., Harvey, M., Malicki, J., Solnica-Krezel, L., Stainier, D. Y., Zwartkruis, F., Abdelilah, S., Stemple, D. L., Rangini, Z. et al. (1996). Mutations affecting the development of the embryonic zebrafish brain. *Development* **123**, 165-178.
Sehnert, A. J., Huq, A., Weinstein, B. M., Walker, C., Fishman, M. and Stainier, D. Y. (2002). Cardiac troponin T is essential in sarcomere assembly and cardiac contractility. *Nat. Genet.* **31**, 106-110.
Shu, X., Cheng, K., Patel, N., Chen, F., Joseph, E., Tsai, H. J. and Chen, J. N. (2003). Na,K-ATPase is essential for embryonic heart development in the zebrafish. *Development* **130**, 6165-6173.
Skinner, D. C. and Caraty, A. (2002). Measurement and possible function of GnRH in cerebrospinal fluid in ewes. *Reprod. Suppl.* **59**, 25-39.
Song, M. H., Brown, N. L. and Kuwada, J. Y. (2004). The cfy mutation disrupts cell divisions in a stage-dependent manner in zebrafish embryos. *Dev. Biol.* **276**, 194-206.
Speake, T., Whitwell, C., Kajita, H., Majid, A. and Brown, P. D. (2001). Mechanisms of CSF secretion by the choroid plexus. *Microsc. Res. Tech.* **52**, 49-59.
Takeyasu, K., Tamkun, M. M., Renaud, K. J. and Fambrough, D. M. (1988). Ouabain-sensitive (Na+ + K+)-ATPase activity expressed in mouse L cells by transfection with DNA encoding the alpha-subunit of an avian sodium pump. *J. Biol. Chem.* **263**, 4347-4354.
Tepass, U. (2002). Adherens junctions: new insight into assembly, modulation and function. *Bioessays* **24**, 690-695.
Therien, A. G. and Blostein, R. (2000). Mechanisms of sodium pump regulation. *Am. J. Physiol. Cell Physiol.* **279**, C541-566.
Vigh, B. and Vigh-Teichmann, I. (1998). Actual problems of the cerebrospinal fluid-contacting neurons. *Microsc. Res. Tech.* **41**, 57-83.
Wei, X. and Malicki, J. (2002). nagie oko, encoding a MAGUK-family protein, is essential for cellular patterning of the retina. *Nat. Genet.* **31**, 150-157.
Westerfield, M. (1995). *The Zebrafish Book: a Guide for the Laboratory Use of Zebrafish*. Eugene, Oregon: University of Oregon Press.
Wiellette, E., Grinblat, Y., Austen, M., Hirsinger, E., Amsterdam, A., Walker, C., Westerfield, M. and Sive, H. (2004). Combined haploid and insertional mutation screen in the zebrafish. *Genesis* **40**, 231-240.
Wright, E. M. (1978). Transport processes in the formation of the cerebrospinal fluid. *Rev. Physiol. Biochem. Pharmacol.* **83**, 3-34.
Yuan, S. and Joseph, E. M. (2004). The small heart Mutation reveals novel roles of Na+/K+-ATPase in maintaining ventricular cardiomyocyte morphology and viability in zebrafish. *Circ. Res.* **95**, 595-603.